

MICROCRACK TOUGHENING: MUTUAL INTERACTIONS  
AND ENERGY DISSIPATIVE MECHANISMS

A. Brencich\* and A. Carpinteri\*

The *process zone* which develops in front of a macrocrack can be simulated by means of a distribution of microcracks; such a simulation has been investigated through a numerical technique based on Displacement Discontinuity Boundary Elements. In the frame of LEFM, which is admissible for brittle materials, the singular stress fields at each crack tip are calculated taking into account also the interactions between the microcracks inside the process zone.

The main features of the interaction phenomena between a main crack and its process zone appear to be independent of the microcrack density. Some considerations about the interactive effects on the main crack tip and on the elastic strain energy absorption give explanation to experimental evidences.

INTRODUCTION

Experimental evidences show that in brittle materials, such as ceramic alloys, a large number of microcracks nucleate in a limited area located just in front of the main crack tip -*process zone*- the orientation of which resembles that of the principal stress directions. In these conditions the material exhibits a macroscopic toughening (Han and Suresh (1), Rühle et al. (2)). From a micromechanical point of view it can be said that the stress field at the main crack tip is shielded both by the elastic interaction between cracks and by the elastic energy release and consequent stress and strain redistribution caused by microcrack nucleation (Hutchinson (3), Shum and Hutchinson (4), Gong (5)). Being the material elastic up to the peak load, a Linear Elastic Fracture Mechanics approach is admissible.

In this work the main crack-microcracks interaction is taken into consideration by simulating the process zone with up to 70 cracks, either oriented as the principal directions or parallel to the main crack line. The elastic problem related to the cracked solid is solved by a numerical procedure based on Displacement Discontinuity Boundary Elements proposed by the authors (Brencich and

---

\* Department of Structural Engineering, Politecnico di Torino, Italy.

Carpinteri (6) which allows to take into account not only the interaction of the main crack with each microcrack but also the mutual interactions between the microcracks. The overall effect on the main crack is addressed via the relative change of the SIF at the main crack tip, and by means of the elastic strain energy distribution between the main crack and the process zone.

### SIMULATION OF THE PROCESS ZONE

The commonly used definition of microcrack density can be given as the ratio between the number of microcracks  $N_V$  ( $N_A$ ) contained in a unit volume  $V$  (unit area  $A$ ) and the volume (area) itself, times the average length  $\langle l \rangle$  cube (square):

$$\rho_V = \frac{N_V}{V} \langle l \rangle^3; \quad \rho_A = \frac{N_A}{A} \langle l \rangle^2. \quad (1)$$

A linear relationship holds between the volumetric and surface microcrack densities, which can be expressed in the form  $\rho_A = \beta \rho_V$ , taking into account that the cracks are not spherical but penny shaped voids, the average value of the coefficient  $\beta$  can be found, Nemati (7):

$$\langle \beta \rangle = \frac{2}{\pi}. \quad (2)$$

The experimental observations on an Alumina-Zirconia alloy (2), on a Silicon-Carbide ceramic alloy (1), and on concrete (7), on the basis of eqs. (1) and (2), give the following estimates for the surface saturated density:

$$\rho_A^{sat} \in [0; 0.10], \quad \rho_A^{sat} \in [0.13; 0.19] \text{ and } \rho_A^{sat} \in [0.02; 0.08]. \quad (3)$$

Once the saturated density is known, and the microcrack length is assumed constant for the sake of simplicity, the crack locations can be obtained so as to simulate different process zones with saturated densities as given in eq. (3). The microcrack distribution is then given a position relative to the main crack tip as if the process zone were generated in the virgin material immediately before the main crack propagation.

For the microcrack orientations two choices have been investigated: an orientation consistent with the principal directions, and another one where all the cracks are parallel to the main crack, represented in figure 1 for different values of the saturated density. The position of the microcrack distribution related to the main crack tip has been indicated as  $\delta$ ,  $\delta=0$  being the position in which the cracks of the process zone are supposed to nucleate, figure 1.

Figure 2 plots the relative variation of the SIF at the main crack tip, which consists of mode I SIF  $K_I$  only for the symmetry of the problem, as a function of the position  $\delta$  of the macrocrack for different saturation densities.

Process zones simulated with horizontal cracks induce stronger amplification and shielding effects than the microcracks oriented along the principal stress directions. Figure 2.b, for example, shows that horizontal cracks amplify the SIF

at the main crack tip three times more than the principal direction oriented cracks. In addition, the shielding effects are only 15% stronger than those induced by oriented cracks, pointing out that microcrack orientation effects are non symmetric with respect to the main crack tip.

Whatever the orientation is, the nucleating position  $\delta=0$  of the microcracks is the one which experiences the strongest amplification, up to 30% of the reference value  $K_{I0}$  for strongly interacting cracks ( $\rho=0.20$ ). It is only the series of relative maxima after the first one that is greatly affected by microcrack orientation: parallel cracks induce an almost unchanged amplification of the main crack, while the oriented cracks induce an overall amplifying effect which is one third of the first maximum. In this case shielding effects remain almost unchanged and lead to a reduction of  $K_I$  which is about 35% less than the reference value.

#### STRAIN ENERGY AND DISSIPATIVE MECHANISMS

When a crack, embedded in an elastic plate, is loaded in mixed mode conditions the elastic strain energy density related to the stress singular field at its tip can be expressed as a function of the SIFs  $K_I$  and  $K_{II}$ , according to Sih (8). It can be proved that the elastic strain energy related to a single crack tip is expressed by the following equation:

$$W_{R^*} = \frac{1+\nu}{8E} \left[ K_I^2 (2\alpha - 1) \sqrt{\frac{1}{8\pi} \left( \frac{K_I}{\alpha} \right)^2} + K_{II}^2 (2\alpha + 3) \sqrt{\frac{1}{8\pi} \left( \frac{K_{II}}{\alpha} \right)^2} \right], \quad (4)$$

where  $\alpha$  represents the limit tangent to the stress function  $\sigma(r)$  for which the asymptotic stress field can be confused with its asymptote, and is set equal to 0.01.

The numerical technique used to investigate the interactive effects allows the computation of the SIFs at each microcrack tip as well as at the main crack one. The total strain energy related to the process zone is obtained summing up the contributions  $W_{R^*}^{mc}$  like eq. (4) of each microcrack tip. The global strain energy  $W_{R^*}^T$  is then obtained adding the contribution due to the main crack  $W_{R^*}^{MC}$ :

$$W_{R^*}^T = W_{R^*}^{MC} + \sum_{mc=1}^{n_{mc}} W_{R^*}^{mc}, \quad (5)$$

where  $n_{mc}$  represents the total number of microcracks.

Figures 3.a and b represent the relative variation of strain energy as a function of  $\delta$ , position between the main crack and the process zone, for  $\rho=0.10$  and  $\rho=0.20$  and either oriented and parallel microcracks. The normalising quantity  $W_0$  is referred to the same geometry in absence of microcracks.

The maximum energy content is related to the position  $\delta = 0$  where the microcracks are supposed to nucleate, while, when the main crack enters the

process zone, the total strain energy decreases: the total strain energy is not constant and it turns out to be a non monotonically decreasing function of  $\delta$ . The total energy content is mainly due to the microcracks, responsible for some 80÷83% of the global strain energy. For parallel cracks the trends are similar, but for a difference which emerges: for  $\delta=0$ , the total energy is not maximum; the maximum strain energy is obtained for the main crack deeply inside the process zone. The total energy is not, in this case, a non monotonically decreasing function.

A comparison between the global strain energy content for different crack orientations is presented in figures 3, bold diagrams, which point out that parallel microcracks are associated to a global elastic strain energy content which is always higher than the energy related to oriented microcracks; for the highest densities it is almost twice the energy absorbed by oriented microcracks.

#### DISCUSSION AND CONCLUSION

The analysis of interactive effects of the process zone on the main crack pointed out that the principal direction orientation of the microcracks lowers the shielding effects on the main crack, but at the same time is responsible of a drop in amplifying effects to one fifth of the value induced by parallel cracks. The microcrack saturated density does not affect the essential features of the phenomenon, being only responsible for the numerical value increase.

The evaluation of the total strain energy related to the main crack-process zone system pointed out that, when the microcracks are oriented like the principal directions, the strain energy content is lower than the energy for parallel cracks, giving a tool for understanding why microcracks nucleate very close to the principal directions. In addition, an important and not trivial observation arises: the energy absorbed by the main crack and the microcracks is not constant by varying the mutual position  $\delta$ . These results altogether give some explanations on the shape and extension of the experimentally observed process zones.

#### REFERENCES

- (1) Han L.X., Suresh S., J. Am. Ceram. Soc., Vol. 72, 1989, pp. 1233-1238.
- (2) Rühle M., Evans A.G., McMeeking R.M., Charalambides P.G., Hutchinson J.W., Acta metall., Vol. 35, 1987, pp. 2701-2710.
- (3) Hutchinson J.W., Acta metall., Vol. 35, 1987, pp. 1609-1619.
- (4) Shum K. M., Hutchinson J. W., Mech. Mater., Vol. 9, 1990, pp. 83-91.
- (5) Gong S. X., Eng. Fr. Mech., Vol. 50, 1995, pp. 29-39.
- (6) Brencich A., Carpinteri A., Int. J. Fract., to appear, 1996.
- (7) Nemati K. M., "Generation and interaction of compressive stress-induced microcracks in concrete", PhD Thesis, Univ. of California at Berkley, 1994.
- (8) Sih G. C., Int. J. Fract., Vol. 10, 1974, pp. 305-321.

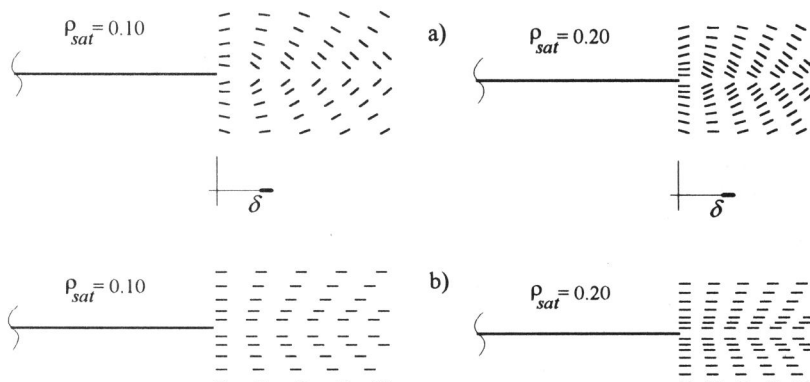


Figure 1: microcracks with different densities and orientations.

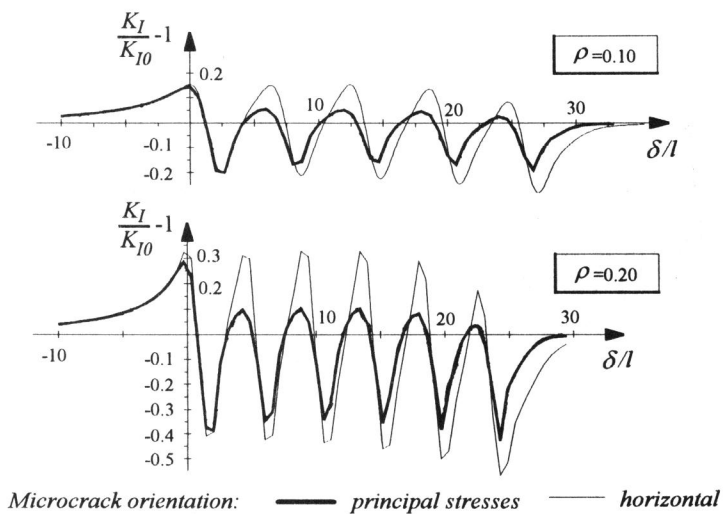


Figure 2: relative variation of the SIF  $K_I$  at the main crack tip as a function of the saturated density and the relative position  $\delta$ .

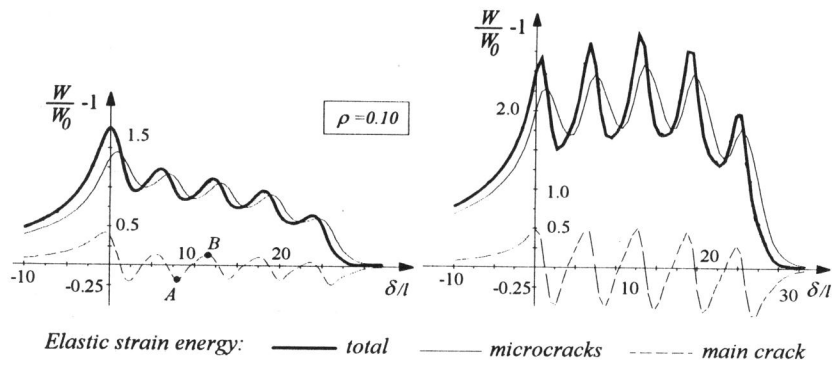


Figure 3.a: strain energy variation as a function of the position  $\delta$ :  $\rho = 0.10$ .

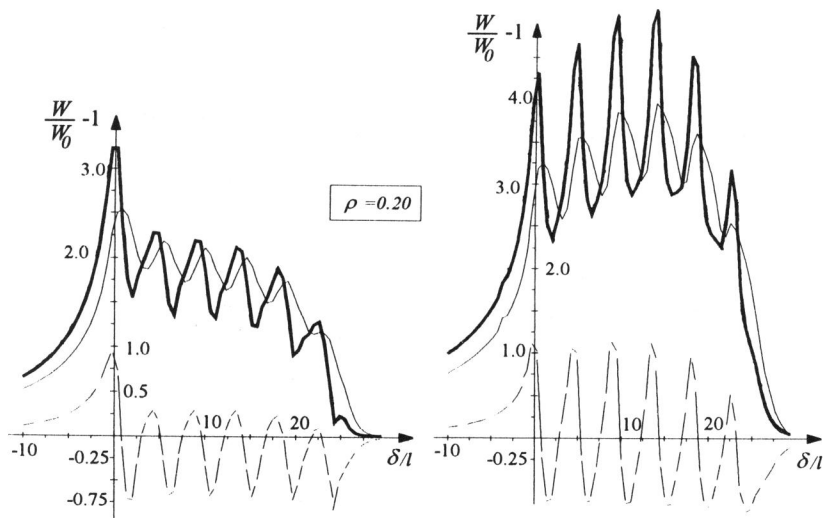


Figure 3.b: strain energy variation as a function of the position  $\delta$ :  $\rho = 0.20$ .